

# Mineralogic variability of the uppermost mantle along mid-ocean ridges

Henry J.B. Dick <sup>1</sup>, Robert L. Fisher <sup>2</sup> and Wilfred B. Bryan <sup>1</sup>

<sup>1</sup> Department of Geology and Geophysics, Woods Hole Oceanographic Institution, Woods Hole, MA 02543 (U.S.A.)

<sup>2</sup> Scripps Institution of Oceanography, University of California at San Diego La Jolla, CA 92093 (U.S.A.)

Received September 15, 1983  
 Revised version received March 27, 1984

Modal analyses of 273 different peridotites representing 43 dredge stations in the Atlantic, Caribbean, and Indian Oceans define three separate melting trends. Peridotites dredged in the vicinity of "mantle plumes" or hot spots have the most depleted compositions in terms of basaltic components, while peridotites dredged at locations removed from such regions are systematically less depleted. The modal data correlate well with mineral compositions, with the peridotites most depleted in pyroxene also having the most refractory mineral compositions. This demonstrates that they are the probable residues of variable degrees of mantle melting. Further, there is a good correlation between the modal compositions of the peridotites and the major element composition of spatially associated dredged basalts. This demonstrates for the first time that the two must be directly related, as is frequently postulated. The high degree of depletion of the peridotites in basaltic major element components in the vicinity of some documented mantle plumes provides direct evidence for a thermal anomaly in such regions—justifying their frequent designation as "hot spots". The high incompatible element concentrations in these "plume" basalts, however, are contrary to what is expected for such high degrees of melting, and thus require either selective contributions from locally more abundant enriched veins and/or contamination by a volatile-rich metasomatic front from depth.

## 1. Introduction

Variously serpentinized and weathered peridotites have been dredged, drilled or sampled by submersible at numerous localities on the walls of fracture zone valleys and also in the rift mountains of slow-spreading mid-ocean ridges like the Mid-Atlantic and Indian Ocean Ridge systems. Many authors have noted the similarity of abyssal peridotites to the alpine-type peridotites located at the base of ophiolite complexes. Such peridotites are believed to be the residues of mantle partial melting which generated the overlying crustal section (e.g. [1–3]). Accordingly, abyssal peridotites are interpreted as residues of mantle melting, depleted in basaltic components and emplaced to the

top of the mantle, finally exposed on the sea floor by faulting of the relatively thin oceanic crust.

Due to the usually high degree of alteration, as well as to the practical difficulty of obtaining materials from the sea floor, abyssal peridotites have been little studied. Assuming a mantle origin, however, their study offers a number of major advantages. Emplaced immediately beneath the crust, these peridotites have undergone the greatest ascent and, therefore, the highest degree of decompression melting of any rocks in the underlying mantle section. Unlike mantle xenoliths, abyssal peridotites dredged from different abyssal localities must share a common petrogenesis; thus it is less critical to sort out their individual high-temperature *P-T* histories. This is particularly important as different pressures and temperatures of equilibration can strongly affect mineral composi-

Woods Hole Oceanographic Contribution No. 5601.

tions. Finally, unlike abyssal basalts, they cannot have been substantially modified by secondary processes such as fractional crystallization, magma mixing and crustal contamination.

Systematic geochemical variations in basalts dredged from the ocean ridges correlate with differences in crestal height and in proximity to mantle hot spots such as Iceland or the Azores [4, and references therein]. Most basalts from the vicinity of presumed hot spots are enriched in incompatible elements, such as K, Rb, Cs, Ba and the light rare earth elements, and have high  $^{87}\text{Sr}/^{86}\text{Sr}$  and low  $^{143}\text{Nd}/^{144}\text{Nd}$  ratios, geochemical features commonly attributed to a mantle source less depleted than the MORB source. In contrast, away from these regions basalts have systematically lower light rare earth and large-ion lithophile element abundances and low  $^{87}\text{Sr}/^{86}\text{Sr}$  and high  $^{143}\text{Nd}/^{144}\text{Nd}$  ratios, features which may be associated with a mantle source which has been previously depleted by extraction of basaltic melts. Morgan [5] proposed that the framework of fixed mantle hot spots, invoked by Wilson [6] to explain the origin of seamount chains and aseismic ridges, is a manifestation of deep mantle plumes bringing heat and relatively primordial mantle material up to the asthenosphere. Morgan's [5] mechanism has in turn been used to explain the geochemical variation of ocean ridge basalts as due to mixing of melts derived from incompatible-element-enriched deep mantle material injected into the upper mantle in the vicinity of hot spots, with melts derived from the depleted upper mantle believed to be the source of "normal" ridge basalts (i.e. [4]). Such models for the origin of ridge basalts require decompression melting accompanying upwelling of the mantle in the upper 100 km beneath ridge axes, and therefore also imply that there may be a compositional variation in the uppermost abyssal mantle complementary to that found in the ridge basalts. To explore this possibility we have undertaken a systematic study of the lateral mineralogical variability of abyssal peridotites along the world ocean ridges relative to spatially associated abyssal basalts, and have examined their proximity to "mantle hot spots". In addition, we consider possible differences in the melting paths for mantle peridotites dredged from the Atlantic, Caribbean

and American-Antarctic Ridges, from the Central Indian Ridge, and from the Southwest Indian Ridge.

## 2. Analytical techniques

Because typical abyssal peridotites contain close to 70–80% alteration products, we use analysis of relict primary minerals and petrographic modal analysis rather than whole rock analyses to interpret the petrogenesis of these rocks. Because alteration products in abyssal peridotites form characteristic pseudomorphs after the primary phases, it is often possible to determine accurately the primary modal phase proportions even when little or no relict primary mineral remains. Roughly half of our dredge hauls or dive stations with peridotites contained material suitable for point counting to obtain such a "primary mode" (Fig. 1). Due to the coarse grain size ( $\sim 0.25\text{--}1.0\text{ cm}$ ) of the rocks, it was necessary to use 7.5 by 5 cm thin sections and to count an average of 2400 points at 1 mm spacing over an area of  $24\text{ cm}^2$  to get a reasonable estimate of the modal proportions (mode) for each sample. In order to assure uniformity, all point counting was done by the first author, with 604,000 points counted on 273 samples from 43 different dredge hauls in the Atlantic, Indian and Caribbean Oceans.

We have mineral composition data for 64 different dredge hauls and dive sites, although this does not include all the locations for which there are modal data. Natural mineral standards, with the exception of one synthetic diopside glass (DJ35), were used for all microprobe analyses. To ensure that the data are representative of the entire sample, olivine and spinel grains from a disaggregated sample were hand picked and mounted on glass slides. From two to six of these grains from each sample were analyzed and averaged for each mineral. To eliminate the effects of low-temperature exsolution, pyroxene analyses were done using glasses fused from hand-picked optically-clear separates of greater than 99% purity. Representative spinel analyses can be found in Dick and Bullen [8]; the remaining analytical data and their detailed interpretation will be published separately.

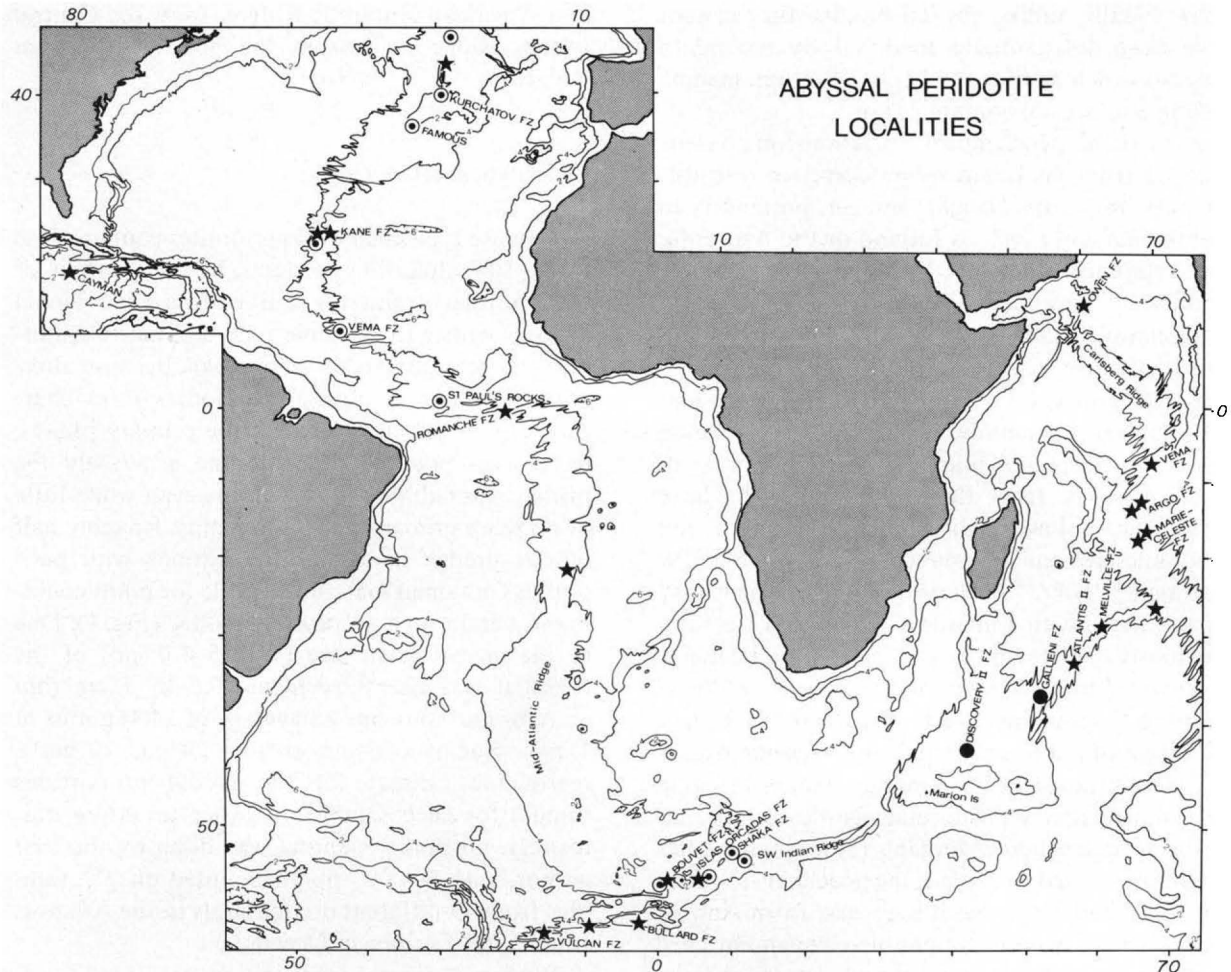


Fig. 1. Map showing distribution of abyssal peridotites used in this study. Stars indicate localities for which there are both modal and mineral data. Filled circles indicate localities for which we have modal data only while open circles indicate localities for which we have only mineral data.

### 3. Modal analyses

An overall average composition for abyssal peridotites, computed by summing the averages for each locality, contains significant plagioclase:  $74.8 \pm 5.3\%$  ( $1\sigma$ ) olivine,  $20.6 \pm 3.7\%$  enstatite,  $3.57 \pm 2.0\%$  diopside,  $0.51 \pm 0.20\%$  spinel and  $0.88 \pm 2.27\%$  plagioclase. This average is deceptive since only about a third of the samples actually contain plagioclase [7,8]. We believe that the plagioclase crystallized late from trapped melt, based on work

on similar plagioclase-bearing alpine-type peridotites [9,10] and from studies of abyssal peridotites [7,8]. Clinopyroxene and plagioclase contents of individual samples in the large suite of unusually plagioclase-rich peridotites from the Romanche Trench show a rough positive correlation consistent with increasing amounts of trapped melt. In addition Dick and Bullen [8] have found that chromian spinels in abyssal plagioclase peridotites contain more ferric iron, as well as higher  $TiO_2$  contents in both pyroxene and spinel, than in

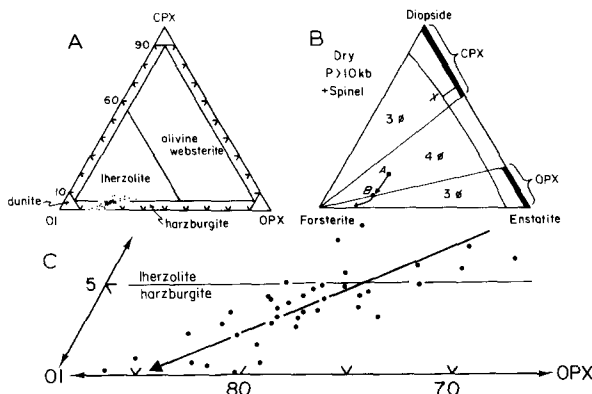


Fig. 2. A. Modal ternary diagram: clinopyroxene-olivine-orthopyroxene with the composition of abyssal peridotites for 39 different dredge hauls plotted using the data in Table 1. Analyses in Table 1 based only on a single peridotite sample have been excluded. Composition fields for different rock types cited in the text are shown for reference. B. Cartoon of the synthetic system  $\text{Mg}_2\text{Si}_2\text{O}_6\text{-CaMgSi}_2\text{O}_6\text{-Mg}_2\text{SiO}_4$ . C. Expanded view of the base of A showing the composition field for abyssal peridotites.

plagioclase-free peridotites. These unique geochemical features can be readily explained as due to the crystallization of trapped melt in the peridotites. In the overall average the high standard deviation for plagioclase relative to the low mean abundance clearly reflects a very non-Gaussian distribution in the sample population; thus we suggest that trapped melt is very irregularly distributed in the mantle at the end of melting. The typical abyssal peridotite in our collections is actually a plagioclase-free spinel-harzburgite containing roughly 75% olivine, 21% enstatite, 3.5% diopside and 0.5% spinel.

There is substantial variability in modal proportions at individual localities, with samples ranging from diopside-poor harzburgites to diopside-rich lherzolites present in the same dredge haul. This local variability is probably equivalent to the outcrop-scale heterogeneities observed in alpine-type peridotites. Such heterogeneities may include local variations in the proportion of mineral phases, flow layering, or the development of patchy dunites within the outcrop. Since the present study primarily concerns the average composition of the local mantle, we have computed an average "mode" for each dredge haul or dive station by

combining all points counted for each mineral on each thin section used (Table 1). These primary modes are plotted (vol. %) in Fig. 2A where it is apparent that there is a systematic variation, with a linear trend away from the enstatite-diopside join toward  $\text{Ol}_{85}\text{Opx}_{15}$ . Although the data are not plotted here, there is also a weak negative correlation between proportions of spinel and olivine (Table 1).

The trend in Fig. 2A can be readily interpreted using the phase relations in the synthetic system  $\text{Mg}_2\text{Si}_2\text{O}_6\text{-CaMgSi}_2\text{O}_6\text{-Mg}_2\text{SiO}_4$ . Fig. 2B is a simplified cartoon of this system. For abyssal peridotites, the modal diagram corresponds only to the four-phase field ( $\text{Ol-En-Di-Sp}$ ) in the cartoon, not the entire synthetic ternary. This is because enstatite in abyssal peridotites is generally saturated with respect to diopside, precluding melting beyond the four-phase field into the three-phase  $\text{Ol-En-Sp}$  field [7]. For any composition in the four-phase field, the composition of the melt is constrained to lie at the reaction point  $X$  until one of the solid phases vanishes. The composition of the residue, with progressive melting, will follow a linear path ( $A-B$ ) directly away from the reaction point towards a "unique" point  $B$  on the olivine-enstatite join. In contrast, melting in the three-phase  $\text{Ol-En-Sp}$  field would produce a path asymptotically approaching the olivine corner of the ternary (path  $B-\text{Fo}$ ). The linear trend for natu-

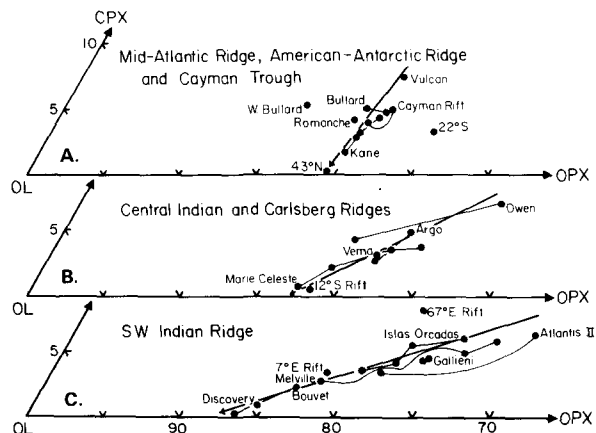


Fig. 3. Expanded view of the olivine corner of the  $\text{Ol-Opx-Cpx}$  modal ternary shown in Fig. 2 with points plotted by region as indicated.

TABLE 1

Modal compositions of abyssal peridotites

Station No.	Lat., long.	Number of samples	Points counted	Olivine (1 $\sigma$ ) <sup>a</sup>	Enstatite (1 $\sigma$ )	Diopside (1 $\sigma$ )	Spinel (1 $\sigma$ )	Plagioclase (1 $\sigma$ )	Locality
<i>Carlsberg Ridge<sup>b</sup></i>									
IN 18	12°35'N, 58°12'E	3	no data	75.2 –	18.8 –	4.30 –	0.27	0.97 –	Owen F.Z.
IN 19	12°36'N, 58°08'E	6	no data	64.5 –	26.8 –	6.85 –	0.88 –	0.35 –	Owen F.Z.
<i>Central Indian Ridge</i>									
CIRCE 93	12°25'S, 65°56'E	5	10,575	81.0 (5.9)	18.1 (5.4)	0.59 (0.95)	0.31 (0.26)	0 –	rift at 12°S, 66°E
ANTP 134	8°42'S, 67°38'E	7	11,923	75.0 (6.7)	21.1 (7.0)	3.41 (1.40)	0.51 (0.28)	0 –	Vema F.Z.
ANTP 135	8°55'S, 67°37'E	3	4088	78.4 (5.1)	20.5 (4.9)	0.71 (0.30)	0.37 (0.57)	0 –	Vema F.Z.
ANTP 125	13°35'S, 66°26'E	4	6771	71.9 (8.2)	22.1 (6.6)	2.76 (1.28)	0.28 (0.19)	3.13 (0.95)	Argo F.Z.
ANTP 126	13°34'S, 66°30'E	4	8632	72.3 (1.9)	22.0 (1.8)	5.10 (2.08)	0.68 (0.29)	0 –	Argo F.Z.
ANTP 84	17°34'S, 65°37'E	7	13,833	73.5 (13.8)	22.5 (9.5)	3.59 (2.35)	0.23 (0.20)	0.23 (0.36)	Marie Celeste F.Z.
ANTP 87	17°36'S, 65°45'E	8	21,229	81.8 (8.2)	17.1 (7.3)	0.73 (1.38)	0.31 (0.32)	0 –	Marie Celeste F.Z.
ANTP 89	17°38'S, 65°49'E	16	36,045	78.7 (4.2)	18.6 (3.4)	2.21 (1.5)	0.32 (0.17)	0.23 (0.36)	Marie Celeste F.Z.
CIRCE 97	17°03'S, 66°52'E	4	9099	72.8 (4.8)	21.3 (4.3)	3.49 (2.31)	0.41 (0.26)	2.02 (1.10)	Marie Celeste F.Z.
<i>Southwest Indian Ridge</i>									
AII107-39	54°27'S, 01°37'E	5	12,909	81.7 (3.9)	16.6 (3.7)	0.51 (0.26)	0.61 (0.18)	0.59 (0.67)	Bouvet F.Z.
AII107-40	54°25'S, 01°34'E	8	17,071	79.4 (2.3)	17.6 (1.8)	2.49 (0.91)	0.50 (0.36)	0 –	Bouvet F.Z.
AII107-35	54°43'S, 00°48'E	1	2763	91.9 –	7.8 –	tr. –	0.30 –	0 –	Bouvet F.Z.
IO11/76-56	54°05'S, 06°17'E	6	12,070	71.5 (1.9)	22.0 (1.9)	5.51 (1.95)	0.91 (0.43)	0.07 (0.17)	Islas Orcadas F.Z.
IO11/76-58	54°04'S, 06°24'E	6	14,698	68.1 (4.5)	25.0 (2.4)	5.93 (2.96)	0.71 (0.29)	0.25 (0.49)	Islas Orcadas F.Z.
IO11/76-59	54°03'S, 06°30'E	6	11,554	73.4 (3.8)	21.7 (4.2)	4.15 (1.30)	0.69 (0.27)	0.01 –	Islas Orcadas F.Z.
IO11/76-60	54°03'S, 06°29'E	13	28,475	75.9 (5.1)	19.8 (3.5)	3.60 (2.08)	0.60 (0.25)	0.06 (0.13)	Islas Orcadas F.Z.
AII107-59	54°01'S, 07°14'E	2	4386	78.3 (0.8)	17.7 (0.2)	3.44 (0.57)	0.46 (0.10)	0.21 (0.34)	Rift at 54°S, 7'E
INMD8-8	41°60'S, 42°39'E	3	7555	84.0 (3.9)	14.4 (3.1)	0.97 (1.62)	0.61 (0.39)	0 –	Discovery II F.Z.
INMD8-15	36°51'S, 52°07'E	8	19,886	71.6 (3.9)	23.4 (3.8)	4.25 (1.45)	0.49 (0.17)	0.31 (0.41)	Gallieni F.Z.
INMD8-12	36°40'S, 52°25'E	5	11,105	71.3 (5.2)	23.7 (4.2)	4.51 (2.08)	0.56 (0.37)	0.04 (0.09)	Gallieni F.Z.
ANTP-114	29°18'S, 60°37'E	3	6108	77.8 (3.9)	18.7 (4.3)	2.85 (0.70)	0.61 (0.30)	0 –	Melville F.Z.

ANTP-115	17°36'S, 65°45'E	7	13,825	69.2 (4.4)	25.4 (3.9)	4.80 (1.47)	0.60 (0.57)	0 –	Melville F.Z.
ANTP-117	30°27'S, 60°48'E	7	15,688	67.0 (2.8)	26.4 (2.4)	5.90 (1.55)	0.53 (0.24)	0.21 (0.64)	Melville F.Z.
AII93-5-2	32°49'S, 56°53'E	2	4884	63.4 (9.8)	29.6 (10.3)	6.18 (0.91)	0.68 (0.39)	0.16 (0.08)	Atlantis II F.Z.
AII93-5-3	32°51'S, 56°55'E	7	16,569	73.2 (4.7)	20.6 (4.4)	3.55 (0.61)	0.22 (0.09)	2.58 (0.84)	Atlantis II F.Z.
AII93-5-9	26°28'S, 67°27'E	4	10,161	69.7 (5.7)	21.6 (2.6)	8.10 (3.61)	0.60 (0.24)	tr. –	Rift at 26°S, 67°E
<i>America-Antarctica Ridge</i>									
Vulc 5-34	57°47'S, 07°40'W	6	12,109	74.9 (3.0)	19.6 (1.8)	4.96 (2.27)	0.56 (0.20)	0 –	NE Bullard F.Z.
Vulc 5-35	57°57'S, 07°49'W	10	21,020	73.6 (4.3)	21.0 (3.3)	4.67 (2.17)	0.69 (0.28)	0.04 (0.32)	NE Bullard F.Z.
Vulc 5-37	58°26'S, 15°40'W	2	3804	78.3 (6.5)	15.6 (2.6)	5.21 (4.26)	0.18 (0.20)	0.66 (0.59)	NW Bullard F.Z.
Vulc 5-41	59°05'S, 16°49'W	12	29,757	70.9 (3.9)	20.8 (2.8)	7.26 (2.53)	0.98 (0.72)	0.03 (0.04)	Vulcan F.Z.
<i>Mid-Atlantic Ridge</i>									
AII60-9	21°56'S, 11°48'W	7	16,640	71.2 (4.0)	24.7 (3.9)	3.19 (1.79)	0.60 (0.32)	0.32 (0.36)	22°S F.Z.
AII20-17	0°03'S, 17°35'W	12	18,206	71.4 (7.6)	18.1 (3.9)	3.89 (2.29)	0.41 (0.28)	6.29 (3.71)	Romanche F.Z.
AII96-1	23°48'N, 46°35'W	8	20,889	76.4 (3.5)	20.1 (3.9)	3.16 (1.42)	0.31 (0.15)	0.03 (0.08)	Kane F.Z.
AII96-2	23°50'N, 46°34'W	4	14,445	74.9 (9.1)	20.3 (6.1)	4.08 (3.42)	0.42 (0.28)	0.30 (0.24)	Kane F.Z.
AII96-10	23°38'N, 44°29'W	2	5384	76.8 (5.2)	20.0 (5.2)	2.79 (0.11)	0.32 (0.17)	0.02 (0.03)	Kane F.Z.
AII96-12	23°38'N, 43°54'W	7	19,622	77.8 (3.3)	19.9 (2.1)	1.76 (1.36)	0.45 (0.12)	0.07 (0.12)	Kane F.Z.
AII32-8	43°13'N, 28°56'W	10	22,134	80.1 (5.3)	19.5 (5.2)	0.16 (0.19)	0.22 (0.20)	tr. –	43°N F.Z.
AII32-10	43°14'N, 29°10'W	1	1737	76.6 –	23.0 –	0.06 –	0.40 –	0 –	43°N F.Z.
<i>Mid-Cayman Rift</i>									
OC23-13	18°10'N, 81°37'W	13	29,985	75.1 (7.5)	20.1 (5.9)	3.91 (2.54)	0.74 (0.51)	0.15 (0.20)	East Wall
OC23-14	18°13'N, 81°33'W	12	23,106	71.2 (8.6)	22.0 (6.9)	4.64 (3.14)	0.68 (0.24)	1.54 (1.44)	East Wall
Total		266	570,740						
Grand Averages [42]			2204	74.80 ± 5.31	20.61 ± 3.67	3.58 ± 2.01	0.51 ± 0.20	0.49 ± 1.16	

<sup>a</sup> Although the mode is computed by summing all the points counted for each mineral on all thin sections from a station,  $1\sigma$  is the standard deviation found for the simple average of the individual modal analyses of each thin section at the station. Thus the quoted mode is the best estimate of the overall mineral proportions at a station, while  $1\sigma$  is an estimate of the total variation of the mineral proportions among the samples from one station.

<sup>b</sup> Data for Carlsberg Ridge from Hamlyn and Bonatti [16].

ral data in Figs. 2a and 2C is thus consistent with variable degrees of melting of roughly similar source rocks in the four-phase field, with the peridotite most depleted in basalt components lying at the olivine-rich end of the trend.

The modal data when plotted by region in Fig. 3 define distinct trends, projecting to separate “unique” points on the  $\text{Ol}-\text{Opx}_{ss}$  join near  $\text{Ol}_{81}\text{Opx}_{19}$ ,  $\text{Ol}_{83}\text{Opx}_{17}$  and  $\text{Ol}_{88}\text{Opx}_{12}$ . We note that none of these trends projects across the  $\text{Cpx}-\text{Ol}$  join, and therefore, unlike the synthetic systems at 10 kbar after which the cartoon in Fig. 3B is modeled (e.g. [18]), clinopyroxene could not have melted incongruently to  $\text{Opx} + \text{melt}$  in the mantle beneath mid-ocean ridges. Although the position of the invariant point  $X$  in Fig. 3B is commonly thought of as “fixed” in composition space, this is only true for the three-component synthetic system  $\text{MgO}-\text{CaO}-\text{SiO}_2$ . Each additional component introduces another degree of freedom, and for the ten major elements required to describe the natural peridotite-basalt system represented by the modal ternary, the position of the invariant point may vary considerably with the initial composition of the mantle. The separate trends (or melting paths) in Fig. 3, therefore, imply that the initial composition of the mantle, and the position of the four-phase invariant point:  $\text{Ol}-\text{Opx}-\text{Cpx}-\text{Sp} + \text{melt}$ , were different for each of these geographic areas.

Additional data from a greater number of localities, however, are needed to substantiate the existence, extent, and variability of the different trends in Fig. 3. The grouping of American-Antarctic Ridge and Mid-Atlantic Ridge peridotites is based simply on the colinearity of the Vulcan and Bullard Fracture Zone peridotites with those from the Kane, Romanche and  $43^\circ\text{N}$  Fracture Zones which is consistent with a similar major element source. The point for the western Bullard Fracture Zone lying off the trend is disregarded as unreliable since it is based on only two samples. The Cayman Trough samples do not define a trend and could lie along any of the other trends. They are shown with the points for the Mid-Atlantic Ridge simply because of the geographic proximity of the two regions. The point for  $22^\circ\text{S}$  is based on 16,640 counts on seven samples and

appears to be reliable. This is the only point for the entire Mid-Atlantic Ridge south of the equator and it lies well off the northern and equatorial Atlantic trend, possibly indicating that the initial mantle composition for this southern region more closely resembled that for the Southwest Indian Ridge.

Examination of the data along the individual trends reveals that, while there may be large differences in the average composition of peridotites dredged at different stations on the same fracture zone, these averages all generally lie along the same trend. This colinearity suggests substantial variations in the amount of melt removed or trapped locally in the upper mantle over a horizontal scale of 1 to 10 km.

Finally, peridotites from (1) the vicinity of so-called “mantle plumes” postulated on the basis of basalt chemistry, apparently anomalous ridge crest elevation, or anomalies in the residual geoid, and (2) peridotites from other regions with basalts from an isotopically less depleted source distinct from “normal” mid-ocean ridge basalt, plot at the depleted olivine rich end of the individual trends in Fig. 3. “Plume” localities include: (1) the Bouvet Fracture Zone, which cuts the Southwest Indian Ridge where it overlies the Bouvet hot spot southwest of South Africa, (2) the Discovery II Fracture Zone, which cuts the Southwest Indian Ridge where it shoals in the vicinity of a well-recognized residual geoid anomaly [11] between the formerly contiguous Del Caño Rise and Madagascar Ridge [12], and (3) the fracture zone near  $43^\circ\text{N}$  on the Mid-Atlantic Ridge, which lies close to the Azores hot spot positioned at  $39^\circ\text{N}$ . Conversely, peridotites dredged from the American-Antarctic Ridge (Fig. 3A), where there is little geophysical evidence for any “hot spot” or “mantle plume” and isotopically enriched basalts with “plume” characteristics are rare compared to MORB (Le Roex, personal communication), plot near the least-depleted, pyroxene-rich end of the trends. So do peridotites dredged from the Melville and Atlantis II Fracture Zones (Fig. 3C) which are located well away from the Del Caño Rise–Madagascar Ridge Sector in a region where the Southwest Indian Ridge is not markedly shallow. Peridotites from four different stations at the Kane

Fracture Zone near 22° N, dredged with “normal” mid-ocean ridge basalt [13], are all enriched in pyroxene compared to the peridotites dredged 1800 km to the north at 43° N near the Azores.

Peridotites collected from the eastern wall of the Islas Orcadas Fracture Zone contain a little over 4% diopside and are substantially richer in pyroxene than the Bouvet Fracture Zone peridotites, although both localities are roughly equidistant from the Bouvet Island Hot Spot. Le Roex et al. [18] have reported the absence of any geochemical gradient along the Southwest Indian Ridge centered on Bouvet Island; instead, “normal”, “plume” and transitional MORB varieties have been dredged in varying amounts for some 800 km along the Southwest Indian Ridge. Basalts recovered from the Islas Orcadas Fracture Zone valley are predominantly “plume” or “transitional” varieties, while those from the adjacent ridge segments, where we have also dredged diopside-rich peridotites, are primarily “normal” MORB [18]. There is, however, an additional fracture zone, the Moshesh, lying between the Bouvet Island hot spot and the Islas Orcadas Fracture Zone which might account for a much reduced “plume” influence in the vicinity of the latter.

We have modal analyses of peridotites from four different areas on the Central Indian Ridge between 8°S and 17°S, in the region now between the formerly-joined elevations of Chagos Plateau and Saya de Malha/Nazareth Bank [14]. These plot toward the pyroxene-depleted, Ol-rich end of the trend defined by Carlsberg and Central Indian Ridge peridotites. Sr isotopic ratios of basalts from this portion of the Central Indian Ridge [15] are slightly high (0.7029–0.7030) and those of associated plutonic rocks somewhat higher; suggesting a mantle source somewhat less depleted than usual for MORB. Crestal depth of the ridge, however, is essentially normal and apparently there is no residual geoid anomaly or other evidence for a hot spot anywhere along the Central Indian Ridge. The majority of peridotites from the Owen Fracture Zone [16] at the northwest end of Carlsberg Ridge near 10°N plot at the undepleted end of the trend. The Carlsberg Ridge displays normal mid-ocean ridge depths;  $^{87}\text{Sr}/^{86}\text{Sr}$  ratios from three basalts from 2°N, 4°N and 10°N on the Carls-

berg Ridge reported by Dupré and Allègre [17] are relatively low (0.7026–0.7028) compared to values from the Central Indian Ridge, and are characteristic of the depleted mantle source of ridge basalts away from postulated mantle “hot spots” and “plumes”. Although there is no geochemical evidence for a hot spot or mantle plume in the region, there is a residual geoid high associated with the Carlsberg Ridge between the equator and 12° N.

If one knew the initial compositions of the mantle parents and the composition of the liquids formed, one could calculate, by using the lever rule, the degree of melting of the abyssal mantle represented by each of the localities lying on the different trends in Fig. 3. Although we do not have this information, making some assumptions about the melt composition allows us to compute a rough estimate of how much additional melting would be required to go from the least to the most depleted locality along the individual trends.

If the position of the liquidus curve for melting of the abyssal mantle is similar to the dry Ol:En cotectic curve of Kushiro [19] for the synthetic system MgO-CaO-SiO<sub>2</sub> at 20 kbar, then to go from the average Melville Fracture Zone peridotite (mean of 3 points in Fig. 3C) to the average Bouvet Fracture Zone peridotite on the Southwest Indian Ridge trend (mean of 2 points in Fig. 3C) requires an additional 17% melting, while to go from the average Vulcan Fracture Zone peridotite to the average 43°N Mid-Atlantic Ridge peridotite on the Atlantic trend (Fig. 3A) would take an additional 11% melting. Using the composition of plagioclase-free olivine websterite bands in Kane and Islas’Orcadas Fracture Zone peridotites (Table 2) (which are possible products of melting) to define the position of the liquidus curve in the modal diagram, it takes an additional 23% melting to go from the Melville to the Bouvet peridotites, and an additional 12% melting to go from the Vulcan to the 43°N peridotites.

Although estimates may vary considerably with choice of initial liquid, the essential point is that the *total variation* in degree of melting suggested by the range of observed peridotite modal mineralogy is large. The variation we find, from around 11 to 23% *additional* melting to go from the least-depleted to the most-depleted abyssal peridotites,

TABLE 2

Modal analyses of olivine websterites

Locality	Olivine	Enstatite	Diopside	Spinel	Counts
<b>Kane Fracture Zone</b>					
AII96-1-3	20.8	43.1	34.3	1.88	2344
<b>Islas Orcadas Fracture Zone</b>					
IO11/76-60-52	28.8	53.2	17.3	0.71	2267

is consistent with the range of estimates from 10 to 30% total melting to form abyssal basalts commonly postulated in the literature.

#### 4. Correlation between mineral and modal compositions

It is important to demonstrate that abyssal peridotites are not simply early residues of fractional crystallization in the crust. One way to do this is to look for a correlation between mineral compositions and modal proportions in the peridotites. A direct correlation between the two is expected if the peridotites are residues of variable degrees of partial melting, as progressive melting must produce a continuous change in both residual mineral compositions and proportions. In contrast, whereas there are systematic changes in the composition of minerals in equilibrium with the melt during progressive fractional crystallization, the crystal path is discontinuous with phases abruptly appearing, disappearing and reappearing on the liquidus. Further, the proportion of phases in a sample of the cumulate residue is highly dependent on relative mineral densities, settling velocities, and the complex fluid mechanics of the magma chamber, so the cumulate mineral phase proportions may not represent assemblages crystallizing at any one time. Thus, a correlation between mineral proportions and composition is neither expected nor generally found in cumulate rocks.

To look for a correlation between mineral modes and composition, we have plotted average Mg/(Mg + Fe) ratios of enstatites, average alumina contents of enstatites, and average Cr/(Cr + Al) ratios of spinels against the average modal proportion of olivine for each of the sixteen localities for

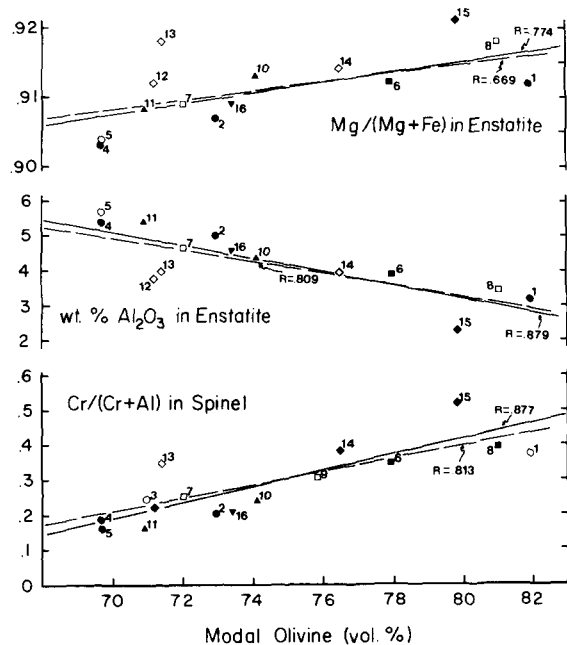


Fig. 4. Binary variation diagrams for abyssal peridotites with mineral compositions plotted against modal olivine averaged by locality. Dashed line is the least-squares fit showing the linear dependence of mineral composition on modal composition for the entire data set.  $R$  = Pearson correlation coefficient. Solid line gives the best fit line for data points (solid symbols) representing more than 3 mineral analyses and 10,000 points counted for the combined modal analysis. Open symbols are for points representing less than 10,000 point counts and less than 4 mineral analyses. Circles are points for the Southwest Indian Ridge: 1 = Bouvet F.Z., 2 = Islas Orcadas F.Z., 3 = Atlantis F.Z., 4 = Melville F.Z., 5 = Rift Valley at 26°S, 67°E. Squares are for the Central Indian Ridge: 6 = Marie Celeste F.Z., 7 = Argo F.Z., 8 = Rift Valley at 12°S, 68°E, 9 = Vema F.Z. Triangles are for the American-Antarctic Ridge: 10 = Bullard F.Z., 11 = Vulcan F.Z. Diamonds are for the Mid-Atlantic Ridge: 12 = 22°S F.Z., 13 = Romanche, F.Z., 14 = Kane F.Z., 15 = 43°N F.Z. The inverted triangle is for the west wall of the Mid-Cayman Rift (16).

which there are sufficient data (Fig. 4). Studies of natural peridotites and melting experiments have shown that these composition parameters are sensitive to variations in degree of melting [20,21]. This reflects the relatively incompatible behavior of alumina and iron, and compatible behavior of chrome in spinel and magnesium in pyroxene. For this purpose only mineral data from plagioclase-free abyssal peridotites are used, as the plagioclase-bearing specimens may be hybrid rocks containing variable amounts of trapped melt. While a small percentage of trapped melt will have a negligible effect on phase proportions in a peridotite, the effect on alumina, titanium and ferric iron contents of the residual minerals is potentially substantial. As can be seen from Fig. 4, there is a strong correlation for each of the mineral composition parameters chosen with the proportion of olivine. As expected, with increasing olivine the spinel  $\text{Cr}/(\text{Cr} + \text{Al})$  and enstatite  $\text{Mg}/(\text{Mg} + \text{Fe})$  increase and the alumina content of enstatite decreases. Thus, most of the variation in mineral chemistry between abyssal peridotite localities can be explained by a model of variable degrees of partial melting of the oceanic mantle.

Some of the scatter in Fig. 4 probably arises from sampling problems; to test for this we recomputed regression lines for the data set, eliminating points representing modes of less than 10,000 points or fewer than four separate analyses of a given mineral. This resulted in regression lines similar to those for the whole data set, but with substantially higher Pearson correlation coefficients (Fig. 4). Some of the scatter in these plots, however, is real; a perfect correlation should exist only if the mantle parent for each locality had the same initial composition. Given the different regional modal compositions trends in Fig. 3, this is unlikely to be the case.

## 5. Mineral and modal composition variations at individual abyssal localities

Hamlyn and Bonatti [16] have reported the absence of any correlation between mineral composition and mineral modal abundance in a peridotite suite from the Owen Fracture Zone. This is

also the case for most of the abyssal peridotite suites we have studied as well. Despite the fact that the average modal analyses for different dredge hauls from the same locality do define a modal trend in Fig. 3 consistent with varying degrees of melting, there is no correlation with average mineral composition (Fig. 5). As can be seen in Fig. 5, whereas there is often a large variation in average modal proportions between dredge hauls from the same locality, there is generally only a small variation in average mineral composition.

Theoretically, both mineral proportions and mineral compositions in the residue of melting in a closed system are strictly controlled by the degree of melting. Although the composition of each mineral within the system will be uniform if equilibrium is maintained and all phases are in contact with the melt, the proportion of mineral phases need not be uniform across the system. In a peridotite, for example, all the pyroxene may be in one area, the olivine in another—although the total proportions of the phases will be fixed within the region melted for a given degree of melting and starting composition. Thus, locally the proportion of the mineral phases may vary considerably and a coherent relationship between mineral compositions and mineral proportions may be found only if the modal composition is measured over an area large enough to represent the total modal composition of the system. Accordingly, for a limited sample, mineral composition is a much better indicator of the regional degree of melting and depletion than mineral mode.

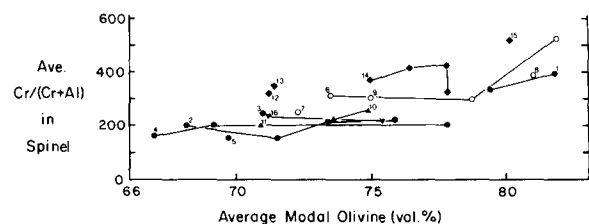


Fig. 5. Binary variation diagram for  $\text{Cr}/(\text{Cr} + \text{Al})$  in spinel plotted against modal olivine content. Similar to Fig. 4, except that data are averaged and plotted for each dredge haul rather than by locality. Points for different dredge hauls from the same locality are connected by tie lines. Symbols and numbers are as in Fig. 4.

If more melt is removed from one area than from another (or trapped at the end of melting), without varying the degree of melting, then the resulting modal variations may still define a coherent melting trend because the proportion of minerals going into the melt is fixed by the four-phase invariant point. Good examples of such trends are defined by the four Kane Fracture Zone dredge hauls (Fig. 3A), the four hauls from the Marie Celeste Fracture Zone (Fig. 3B) and the four hauls from the Islas Orcadas Fracture Zone (Fig. 3C). In each of these cases it would appear that melt either did not form and segregate uniformly or was not uniformly trapped at the end of melting across the locality, resulting in the observed modal heterogeneity. Thus the linear trends in Fig. 3 for individual localities can be interpreted, in part, as simple addition-subtraction lines for varying proportions of trapped melt and residue at the end of melting.

Thus we interpret the absence of a correlation between mineral modes and chemistry at individual abyssal peridotite localities as indicating a simple one-stage melting history, with variable degrees of melt removal at the end of melting. This does not, of course, rule out progressive or dynamic melting during ascent. In contrast Dick [20] has found good correlations between mineral modes and chemistry across 30 km of a single alpine-type peridotite together with evidence for at least two separate, unrelated, melting events.

## 6. Correlation between peridotite modal compositions and the normative composition of associated basalts

We believe that we have adequately demonstrated that abyssal peridotites are residues of variable degrees of mantle melting. However, if it can be demonstrated that these variations are related to compositional variations in basalts dredged from the same regions, this would further strengthen the interpretation that the peridotites are the residues of ridge basalt generation. An alternate explanation for the linear modal trends in Fig. 3, and for the correlations between mineral modes and major element compositions in Fig. 4,

is that the degree to which melt is removed from the mantle, rather than the degree of melting, is varying. Such an explanation, however, cannot explain the observed variations in the peridotites if these correlate with variations in the composition of the spatially associated basalts. This is because melt composition may vary with the degree of melting but not with the amount tapped off at the end of melting.

There is a sampling problem when attempting

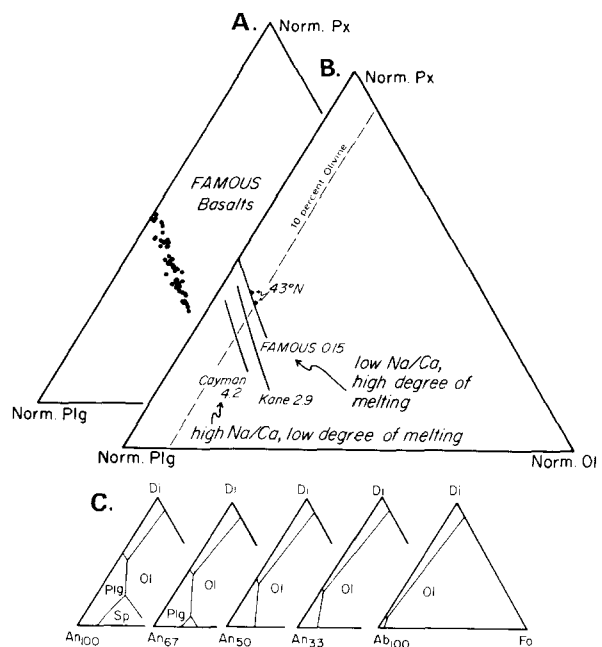


Fig. 6. A. Normative plagioclase-olivine-pyroxene ternary showing the composition of basalt glasses from the FAMOUS region of the Mid-Atlantic Ridge from Bryan and Moore [22]. Norms are calculated with all iron as FeO. B. Best fit line for the data in Fig. 6A and best-fit lines for natural basalt glasses from the Mid-Cayman Rift and the Kane Fracture Zone region from Bryan and Dick [24]. Compositions of two basalt glasses published by Shibata et al. [38] for 43°N are shown for reference. Number besides locality name gives the modal diopside content of spatially associated dredged peridotites (data from Table 1). Dashed line is that of constant 10% normative olivine. C. Phase relations in the system albite-anorthite-diopside-forsterite determined for starting materials with different Ab/(Ab+An) ratios from Biggar and Humphries [25]. Note that this system contains five components (CaO, MgO, Al<sub>2</sub>O<sub>3</sub>, SiO<sub>2</sub>, Na<sub>2</sub>O) and is therefore only an approximate analog for the 10+ component natural systems in Figs. 6A and B.

to compare dredged basalts and peridotites. The basalts occasionally recovered with peridotites in a single haul commonly are badly altered. Generally one has to rely on material from other hauls often located on the axis of the nearby ridge but still some tens of kilometers away from the peridotite locality. Since the dredged basalts may have been erupted over a fairly wide temporal and spatial range, it is unlikely that any have actually been derived from the particular peridotites studied. In one sense, this is an advantage in that any correlation is essentially "regional", demonstrating that the small sub-sample acquired by dredging may be representative of a large area, with peridotites dredged from a fracture zone or rift mountain related to the basalts erupted on the nearby ridge.

Geochemists generally have looked for evidence for mantle source variations in the trace element or isotopic compositions of basalts. This is in large part because the major element composition of basaltic melts can be substantially modified after separation from the mantle source due to processes such as wall rock assimilation, magma mixing and fractional crystallization. In order to relate the major element compositions of basalts and spatially associated peridotites, therefore, we use the position of the liquid line of descent in the norma-

tive olivine-plagioclase-pyroxene ternary defined by the compositions of natural basalt glasses dredged from a region (see Fig. 6). Fig. 6A is a ternary plot of glasses dredged from an extensive area ( $\sim 700 \text{ km}^2$ ) around the FAMOUS region of the Mid-Atlantic Ridge. Despite the fact that the glasses represent a wide spatial and temporal range [22], they all plot close to a single line which defines the crystallization path for basalts from the region and mimics the olivine-plagioclase cotectic boundary in the synthetic system anorthite-diopside-forsterite [23]. Regression lines computed for the FAMOUS glasses and for glasses from some other regions (Fig. 6B) show obvious differences [24]. Schilling et al. [4] also have shown that in the North Atlantic in general basalts and basalt glasses from individual areas follow unique trends and collectively define a family of cotectic trends. The close fit of pillow basalt glasses from a given region to a single line must mean either that the primary melts separating from the mantle over a considerable spatial and temporal range are highly uniform with respect to major element composition, or that different melts are derived in relatively constant proportions from the mantle and are well mixed prior to eruption.

Fig. 6C portrays a summary of recent experi-

TABLE 3

Major element compositions and critical major element ratios of representative basalt suites at about 10% ternary normative olivine [23]

	Cayman	Kane	FAMOUS	Cayman/FAMOUS
<i>Major elements (wt.%)</i>				
SiO <sub>2</sub>	51.65	50.57	49.82	
TiO <sub>2</sub>	2.27	1.69	0.84	2.7
Al <sub>2</sub> O <sub>3</sub>	15.09	15.57	16.23	
FeO	10.46	10.29	9.07	
MgO	5.68	7.27	9.19	
CaO	9.37	11.02	12.22	
Na <sub>2</sub> O	4.06	3.00	2.06	
K <sub>2</sub> O	0.27	0.14	0.09	3.0
P <sub>2</sub> O <sub>5</sub>	0.26	0.18	0.10	2.7
Na <sub>2</sub> O/CaO	0.43	0.27	0.17	
Norm Ab/An	0.608	0.470	0.334	
Olivine	9.90	9.70	10.07	
Plagioclase	60.88	56.66	53.67	
Pyroxene	29.72	33.64	36.26	

mental work in the system An-Ab-Di-Fo where phase relations were mapped in the Ol-Plg-Px ternary using a range of albite/anorthite ratios in the starting materials [25]. As the initial Ab/An ratio increases, the plagioclase-olivine cotectic shifts to the left across the ternary diagram. Consistent with this, the Na/Ca ratio of representative FAMOUS, Kane, and Cayman basalts for roughly constant normative olivine contents, increases systematically from 0.17 to 0.43 with increasing concentrations of other incompatible elements, including  $K_2O$ ,  $P_2O_5$ , and  $TiO_2$  (Table 3). The initial Fe/Mg ratio of the parent melt might also be a factor in fixing the position of the regional basalt liquidus trend. The effect is not likely to be as significant as the Na/Ca ratio, however, since the Fe/Mg ratios of abyssal peridotites, and therefore the Fe/Mg ratios of the derived primary magmas, show little variation [7].

In order to test whether the shift of the basalt liquidus trends might be related to regional variations in the composition of the underlying mantle, each of the trends in Fig. 6B has been annotated with the proportion of modal diopside in spatially associated dredged peridotites. The proportion of residual diopside in the peridotites increases systematically, indicating that the residual mantle becomes less depleted in diopside as the natural basalt liquidus trends shift to the left in the ternary diagram. This correlation is consistent with changes in the mineralogy of the peridotites during melting. Sodium, held largely in the pyroxene as jadeite component, is related to the large-ion lithophile elements, and generally behaves incompatibly during melting, while calcium is a major stoichiometric component of pyroxene, which must decrease in the residue and go into the melt only as residual pyroxene decreases. Thus, while the concentration of sodium in the melt decreases steadily with increasing melting, calcium must remain nearly constant. The Na/Ca ratio of the melt (and hence Ab/An), then, should systematically decrease as more pyroxene melts, and, as one finds in Fig. 6B, the corresponding ridge basalt liquidus trend should shift to the right in the Ol-Plg-Px ternary towards pyroxene as diopside decreases in associated residual mantle peridotites. Another way of looking at this effect is to realize that plagioclase

component exists in the peridotites largely in the jadeite and Tschermark molecules in pyroxene. As jadeite molecule is largely removed from the pyroxene at the early stages of melting and Tschermarks is preferentially removed throughout melting, the residue is effectively depleted in potential plagioclase component relative to diopside component and as fusion proceeds the plagioclase/pyroxene and Na/Ca ratios of the melt must decrease.

Although we have used normative phase proportions calculated from glass chemical analyses to define these liquidus trends, the reality of these differences in phase proportions is confirmed by petrography and modal analyses of selected basalts. Schilling et al. [4] and Schilling and Thompson [26] have shown that modal phenocryst pyroxene is characteristic of basalts associated with "hot spots", as especially demonstrated near the Galapagos, the FAMOUS area, and Iceland. Bryan [27] subdivided modal phenocryst data according to association of the basalt with "normal" incompatible-element-depleted ridge segments (Group I) or with incompatible-element-enriched ridge segments (Group II). He showed that in the Group I basalts modal phenocryst pyroxene only appears among the highly phryic basalts, generally associated with highly fractionated glasses. In the Group II basalts, from "hot spot" regions, phenocryst pyroxene appears at low degrees of crystallization and in association with relatively unfractionated glasses. Thus, the differences in phase saturation implied by the normative data are confirmed by the natural modal phase assemblages appearing as phenocrysts in the basalts.

To test our model on a larger scale, we have plotted the plagioclase/(plagioclase + pyroxene) ratios where the basalt liquidus trends cross 10% normative olivine (dashed line in Fig. 6B) against the amount of modal diopside in spatially associated peridotites for 13 localities for which we have sufficient data (Fig. 7). There is a strong correlation, with only one locality (the ridge crest at 12°S) falling significantly below the general trend. The Bouvet Fracture Zone is anomalous in that three separate liquidus trends are defined by basalt glasses dredged to the east and west of the fracture zone (Dick, unpublished data). Assuming that the

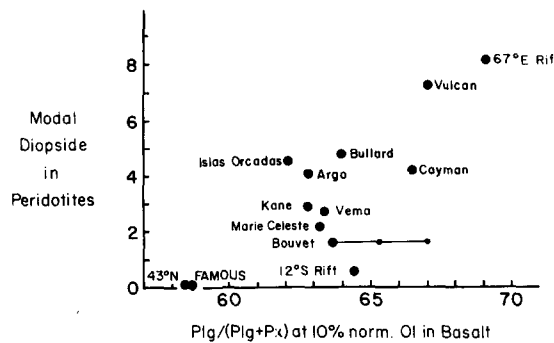


Fig. 7. Modal diopside content of abyssal peridotites plotted against the plagioclase/(plagioclase + pyroxene) ratio of spatially associated abyssal basalt glasses at a constant normative olivine content of 10% (intersection of natural basalt liquidus trend and dashed line in Figure 5). Glass data sources: FAMOUS—Bryan and Moore [22]; Kane F.Z.—Bryan et al. [13]; 43°N—Shibata et al. [38]; Cayman Rift—Thompson et al. [39]. All other data are from unpublished work by Dick on South Atlantic basalts in the Woods Hole Oceanographic Institution collection and Indian Ocean basalts from Scripps Institution of Oceanography dredge collections.

different Spies Ridge cotectic trends are due to sequential melting of the underlying mantle, it is important to note that the liquidus trend representing the highest degree of melting according to our model does fit the overall correlation in Fig. 7. It is apparent, then, that the position of the basalt liquidus trends in the normative Ol-Plg-Px ternary directly reflects the degree of melting of the immediately underlying source region.

## 7. Hot spots, the geoid, and mantle peridotites

A principal feature believed related to “mantle plumes” is an upward deflection of topography and the earth’s geoid. The variations in the geoid are often of sufficiently large wave length (> 500 to 1000 km) that it is unlikely that they could be maintained by elastic stresses in the lithosphere (e.g. [28]). Theoretically they could most easily be maintained dynamically by upward motions in the mantle and the associated thermal anomaly; they have been interpreted and modelled as such by a number of authors (e.g. [29,30]). Locally, we find a good correlation between geoid height and the

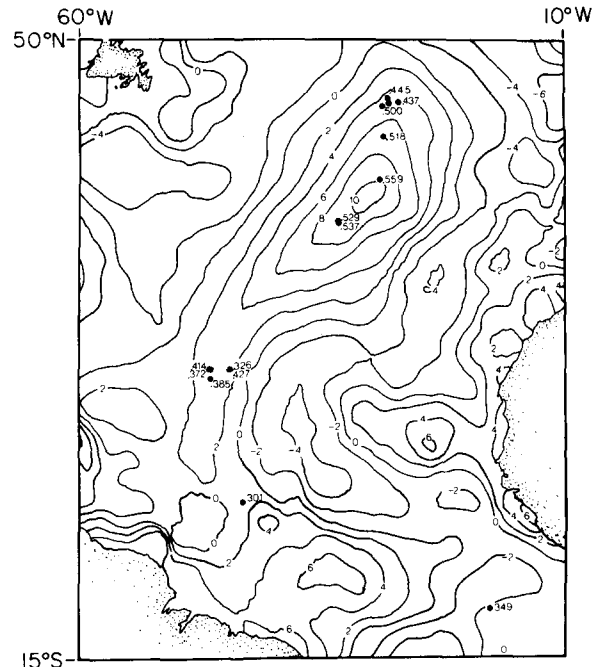


Fig. 8. Geoid anomaly map of the North Atlantic contoured at 1-m intervals from Parsons et al. (in preparation) with the  $\text{Cr}/(\text{Cr} + \text{Al})$  ratio of spinel in dredged abyssal peridotites plotted on it. Additional data sources: DSDP Site 395—Sinton [40]; Vema F.Z.—Hamlyn and Bonatti [16]; 45°N—Aumento and Loubat [41].

composition of dredged peridotites. In Fig. 8 we take the average  $\text{Cr}/(\text{Cr} + \text{Al})$  ratio of spinel in dredged peridotites as an index of the degree of melting and plot this compositional parameter on an anomaly map of the geoid between 50°N and 15°S in the Atlantic from M. Roufosse [11]. Spinel  $\text{Cr}/(\text{Cr} + \text{Al})$  is used as there is substantial additional data for spinel in North Atlantic peridotites available in the literature and as this parameter is particularly sensitive to variations in degree of melting [8]. The most prominent feature of the geoid topography in this region is the large positive anomaly near 40°N associated with the Azores triple junction. As shown here, the  $\text{Cr}/(\text{Cr} + \text{Al})$  ratio of spinel in peridotites dredged along the Mid-Atlantic Ridge increases systematically with the geoid height, increasing from a minimum of 0.301 to the south at the Vema Fracture Zone where the geoid anomaly is close to 0, to a maximum of 0.559 at the Kurchatov Fracture Zone

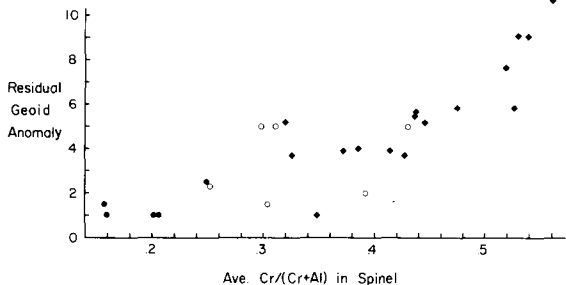


Fig. 9. Cr/(Cr + Al) of spinel in dredged peridotites from this study versus the height of the residual geoid in meters from Parsons et al. (in preparation).

near the apex of the Azores anomaly, dropping again to 0.445 further north.

A number of features other than putative mantle plumes associated with hot spots, however, contribute to geoid topography; overall a plot of all our data against geoid height around the world produces only a rough correlation. Thus to examine the possible relationship between hot spots and the composition of dredged peridotites, it is better to use the residual geoid after the topographic contribution due to the ocean ridges is removed. Hence in Fig. 9 we plot the average Cr/(Cr + Al) ratio of spinel at a locality against the height of the residual geoid as calculated for the world by Parsons et al. (in preparation). This gives a good correlation, suggesting that a large proportion of the petrologic variation in abyssal peridotites may be accounted for by the same factors giving rise to "mantle hot spots".

Removing the effect of the ridges shifts the central North Atlantic geoid high to the east, directly over the Azores Islands (B. Parsons, personal communication and [30]). This is significant as the mantle peridotites dredged in the vicinity of the ridge axis to the west show the effect of the Azores hot spot. This implies significant sub-lithospheric transport of heat and material westward from the Azores region, against the mantle flow lines associated with plate spreading in the region. Schilling and Thompson [26] report similar observations and conclusions based on the isotopic and trace element composition of ridge basalts dredged to the west of Ascension, St. Helena, Tristan da Cunha and Gough Islands in the South Atlantic.

## 8. Summary and conclusions

The data presented here for abyssal peridotites from six mid-ocean ridges show correlations between modal mineralogy and mineral composition consistent with interpretation of the regional differences between these rocks as being due to variable degrees of mantle melting. Overall the total variation appears to be large, with approximately 15% additional melting required to go from the least- to the most-depleted mantle peridotite. We find further correlations between the composition of abyssal peridotites, the position of liquidus trends for spatially associated basalts, and the proximity of these rocks to presumed "mantle plumes". This provides the first direct evidence for the commonly inferred direct genetic relationship between abyssal basalts and the immediately underlying residual mantle, with the highest degree of melting leaving the most-depleted mantle in the vicinity of mantle hot spots.

The simplest interpretation of the compositional variation of abyssal peridotites along ocean ridges is that the degree of melting of the shallow mantle in the region of so called "mantle plumes" is close to a factor of two or three greater than in areas where a mantle plume influence is absent. This requires a large thermal anomaly in the mantle in these areas, justifying their designation as "hot spots", with far more heat available for melting, as predicted by the mantle plume hypothesis of Morgan [5] and inferred by geophysical modelling of the geoid in these regions. This is the first direct evidence for such a thermal anomaly other than the geoid anomaly itself \*. In addition, the high degree of depletion in basaltic components of

\* We would like to note here that Dr. Peter Michael, working at Lamont-Doherty with Dr. Enrico Bonatti, has also identified the zone of anomalously depleted abyssal upper mantle in the North Atlantic previously identified by Dick and Fisher [7], and has interpreted this anomaly as associated with the Azores mantle plume. This latter conclusion was reported simultaneously during papers given at the AGU meeting in Spring 1983 [31,32]. The two studies appear to substantiate each other, as in large part the samples studied were from different localities. In addition, Langmuir and Hanson [33] identified a zone of anomalously major-element-depleted mantle in the same region of the North Atlantic on the basis of basalt compositions.

residual abyssal peridotites near hot spots would appear to rule out small degrees of melting as a petrologic mechanism for generating "plume" ridge basalts where they are the predominant magma type.

Because high degrees of melting would be expected to result in lower concentrations of incompatible elements in liquids derived from a given source, the "enriched" trace element and isotopic chemistry of the basalts dredged in "hot spot" regions seems to require very substantial differences in source between hot spots and normal ridge segments. The linear regional trends seen in Figs. 2 and 3, on the other hand, seem to imply a common mantle parent in terms of major elements for large regions encompassing areas of both P- and N-type ridge basalts, with principal differences arising due to the varying degrees of melting.

Schilling et al. [4] have shown that North Atlantic MORB tend to lie along discrete cotectics, as noted by Bryan and Dick [24]. Some basalt groups adjacent to Iceland are displaced to even higher pyroxene/(pyroxene + plagioclase) ratios than FAMOUS. Because their data are whole-rock analyses, there may be some scatter due to phenocryst accumulation and a rigorous comparison to our glass data may be inappropriate. However, their data suggest that variable cotectics are found among plume-related basalts, among basalts from transitional ridge segments, and in basalts from normal ridge segments. Thus, if differences in these trends are due to differences in degree of melting of the mantle source, these data suggest that variable melting is common along spreading ridges and that, while high degrees of melting do seem characteristic of "hot spots", some other factor must account for the large enrichments in incompatible trace elements also found there. Thus, it seems almost essential to postulate that the high degrees of melting at "hot spots" associated with ocean islands and platforms are a consequence of a rising thermal and metasomatic front, which adds volatile components and incompatible elements to the mantle (i.e. [4]). Such a front, enriched in P, K, Ti, and light rare earth elements as well as volatiles, would not strongly affect the local major element composition of the mantle but would significantly

modify the trace element composition of the derived basalts, depress the mantle melting point, and make additional heat available for melting from below.

Rare earth element studies of mantle xenoliths would appear to have a direct bearing on the problem outlined above. A decoupling of incompatible trace element (K, P, U, LREE) abundances and CaO-Al<sub>2</sub>O<sub>3</sub> abundances has been found to exist in nearly all xenolith suites studied in detail [34]. Specifically as xenolith suites go from relatively major-element-undepleted lherzolites to relatively major-element-depleted harzburgites, the absolute abundance of the heavy rare earths decrease and the xenoliths became light-rare-earth-enriched relative to the heavy rare earths. Frey and Green [35], in a widely accepted interpretation, suggested that the lherzolites and harzburgites were comprised of two components: one which determined the major element and compatible trace element composition, and one which determines the abundance of minor and incompatible trace elements including K, P, LREE, Th and U. They have suggested that these consist of a partial melting residue which is modified by the addition of a genetically unrelated migrating (metasomatic) fluid.

The observations of Frey [34] and others are in fact similar to ours, except that we find the most major-element-depleted mantle peridotites spatially associated with the most LREE and incompatible-element-enriched basalts along mid-ocean ridges. We would suggest therefore that our preferred hypothesis, though similar to Frey and Green's [35], better explains the data for both xenoliths and oceanic peridotites. Frey and Green's [35] hypothesis, as it stands, leaves the systematic increase in LREE in the xenoliths with increasing degree of depletion in major elements as the result of fortuitous mixing of two unrelated components. In light of the evidence of Dick [20] that melt may be trapped in mantle peridotites at the end of melting, we suggest that the degree of melting is being controlled largely by the amount of metasomatic fluid introduced at the beginning of melting. At the end of melting, the most-depleted harzburgites will show the strongest enrichment in LREE, reflecting the composition of the trapped melt.

Another explanation is that metasomatic and other types of veins in the mantle, enriched in various incompatible and radiogenic isotopes, are in large part removed from an otherwise depleted mantle by early melting in an ascending mantle plume. While the remaining relatively depleted deep mantle material spreads laterally into the upper mantle beneath and along the ridge, the early formed melts, for the most part, ascend directly above the plume. As one moves down the ridge, away from the axis of a hot spot, less of this early melt is available to mix with later melts formed as the depleted mantle ascends between the separating lithospheric plates. Similar models of melting of a variably veined mantle have been previously proposed [20,36,37]. This model explains why mantle sampled beneath a plume and that sampled away from the plume lie on the same melting trend, but may differ in incompatible element enrichments, and why the degree of melting of the mantle emplaced in a hot spot region is greater; both the thermal anomaly associated with the plume, and an abundance of early formed enriched melt rising into a region from below, will promote greater degrees of local mantle melting. The weakness of this model lies in the degree to which the vein and country rock assemblages can be maintained as isotopically distinct reservoirs over periods of up to 2 b.y. as appears to be required by the differences in the isotopic signatures of MORB and plume basalts [42]. This is not, of course, a problem for the metasomatic model. Although the different melting trends shown for different oceanic regions in Fig. 3 require further substantiation, they coincidentally fit well with the regional variations for oceanic island basalt sources identified by Dupré and Allègre [17]. Those authors found that, in terms of Nd-Sr-Pb isotopic compositions, rocks from oceanic islands in the Indian Ocean and the eastern South Atlantic have a mantle source distinct from that for North Atlantic and eastern Pacific oceanic island basalts. If the source of the oceanic island basalts is the same as for the plume component of ridge basalts near hot spots, then it would seem that the America-Antarctic Ridge region may belong to the latter source region, as peridotites from this ridge lie on the North Atlantic melting trend.

A major constraint on any model explaining the lateral chemical variability of mid-ocean ridge basalts is the lack of chemical gradients where the very slow-spreading Southwest Indian Ridge crosses the putative Bouvet mantle plume. There “plume”, “normal” and “transitional” mid-ocean ridge basalts were recovered, often in the same dredge haul, for some 800 km along the Southwest Indian Ridge. In addition, Le Roex et al. (in preparation) have found that rare “plume” and “transitional” basalts also occur along the very slow-spreading American-Antarctic ridge in small amounts with far more abundant “normal” mid-ocean ridge basalts; these are far from any postulated mantle plume. This suggests that geochemical gradients such as those reported in the vicinity of Iceland and the Azores (e.g. [4]) are present only where the spreading rate and hence the magma production rate is large enough that different batches of basalt derived from a heterogeneous mantle undergo sufficient mixing to cause local homogenization—presumably in a shallow magma chamber. The generation of ridge basalts, therefore, may require sequential melting of a heterogeneous or variably veined mantle (e.g. [18]) or variable contamination of a more uniform mantle by metasomatic fluids derived from a relatively undepleted source deep in the mantle.

We consider the most likely metasomatic fluid to be a silicate melt. What we have examined to date in this paper are correlations between the net product and net residual of these processes. The correlation between the position of the basalt liquidus trend and average degree of major element depletion of spatially associated residual peridotites demonstrates only that these residual peridotites dominated the major element chemistry of the “homogenized” basalt product both close to and away from mantle plumes. It does not rule out the localized generation of large-ion element-enriched basalts by small degrees of melting in a region. The “plume” basalt recovered along the American-Antarctic Ridge, for example, could be exactly such products. These fine-scale complexities obviously require further examination.

## Acknowledgements

Field and laboratory work for this study were supported by National Science Foundation grants Nos. DPP-7721208 and DPP-8019769 to the Woods Hole Oceanographic Institution and DES74-02474 to the Scripps Institution of Oceanography, in addition to Office of Naval Research contracts Nos. N00014-75-C-0152 and N00014-80-C-0440 with Scripps Institution of Oceanography. Barry Parsons made gravity field interpretations available before publication, as well as thoughtful suggestions. F.B. Wooding, M. Otter, and T. Bullen of the Woods Hole Oceanographic Institution provided technical assistance and aided in microprobe analysis. S.A. Morse, S.R. Hart, C.H. Langmuir, G. Thompson, J. Natland and P. Meyer provided provocative and useful reviews of the manuscript. Anton Le Roex provided access to unpublished isotopic data for American-Antarctic Ridge basalts as well as many specific comments which greatly improved the manuscript.

## References

- 1 A. Miyashiro, F. Shido and M. Ewing, Composition and origin of serpentinites from the Mid-Atlantic Ridge near 24° and 34° north latitude, *Contrib. Mineral. Petrol.* 23, 117, 1969.
- 2 E. Bonatti, J. Honnorez and G. Ferrara, Equatorial Mid-Atlantic Ridge: petrologic and Sr isotopic evidence for an alpine-type rock assemblage, *Earth Planet. Sci. Lett.* 9, 247, 1970.
- 3 G.B. Udrinsev and L.V. Dmitriev, Ultrabasic rocks, in: *The Sea*, 4, Part 1, 521, 1971.
- 4 J.-G. Schilling, M. Zajac, R. Evans, T. Johnston, W. White, J.D. Devine and R. Kingsley, Petrologic and geochemical variations along the Mid-Atlantic Ridge from 29°N to 73°N, *Am. J. Sci.*, pp. 510-586, 1983.
- 5 W.J. Morgan, Convection plumes in the lower mantle, *Nature* 230, 42, 1971.
- 6 J.T. Wilson, Evidence from ocean islands suggesting movement in the earth, in: *A Symposium on Continental Drift*, P.M.S. Blackett, E. Bullard and S.K. Runcorn, eds., *Philos. Trans. R. Soc. London, Ser. A*, 258, 145, 1965.
- 7 H.J.B. Dick and R.L. Fisher, Mineralogic Studies of the residues of mantle melting, in: *Proceedings of the Third International Kimberlite Conference, Developments in Petrology*, Elsevier (in press).
- 8 H.J.B. Dick and T. Bullen, Chromian spinel as a petrogenetic indicator in abyssal and alpine-type peridotites and spatially associated lavas (submitted *Contrib. Mineral. Petrol.*).
- 9 F. Boudier and A. Nicolas, Structural controls on partial melting in the Lanzo Peridotite, in: *Magma Genesis*, H.J.B. Dick, ed., Oreg. Dep. Geol. Miner. Ind. Bull. 96, 63, 1977.
- 10 W.R. Church and R.K. Stevens, Early Paleozoic, ophiolite complexes of the Newfoundland Appalachians as mantle-ocean crust sequences, *J. Geophys. Res.* 76, 1460, 1971.
- 11 M. Roufosse, B. Parsons, D. McKenzie and T. Watts, Geoid and depth anomalies in the Indian Ocean (Abstract), *EOS, Trans. Am. Geophys. Union* 62, 289, 1981.
- 12 R.L. Fisher and J.G. Sclater, Tectonic evolution of the Southwest Indian Ocean since the Mid-Cretaceous: plate motions and stability of the pole of Antarctica/Africa for at least 80 million years, *Geophys. J. R. Astron. Soc.* 73, 552, 1983.
- 13 W.B. Bryan, G. Thompson and J. Ludden, Compositional variation in normal MORB from 22-25°N, Mid-Atlantic Ridge and Kane Fracture Zone, *J. Geophys. Res.* 86, 836, 1981.
- 14 R.L. Fisher, J.G. Sclater and D.P. McKenzie, Evolution of the Central Indian Ridge, western Indian Ocean, *Geol. Soc. Am. Bull.* 82, 553, 1971.
- 15 C.E. Hedge, C.E. Futa, C.G. Engel and R.L. Fisher, Rare earth abundances and Rb-Sr systematics of basalt, gabbro, anorthosite, and minor granitic rocks from the Indian Ocean ridge system, western Indian Ocean, *Contrib. Mineral. Petrol.* 68, 373, 1979.
- 16 P.R. Hamlyn and E. Bonatti, Petrology of mantle-derived ultramafics from the Owen Fracture Zone, northwest Indian Ocean: implications for the nature of the oceanic upper mantle, *Earth Planet. Sci. Lett.* 48, 65, 1980.
- 17 B. Dupré and C.J. Allègre, Pb-Sr isotope variation in Indian Ocean basalts and mixing phenomena, *Nature* 303, 142, 1983.
- 18 A.P. Le Roex, H.J.B. Dick, A.J. Erlank, A.M. Reid, F.A. Frey and S.R. Hart, Geochemistry, mineralogy and petrogenesis of lavas erupted along the SW Indian Ridge between the Bouvet Triple Junction and 11 degrees east, *J. Petrol.* 24, 267, 1983.
- 19 I. Kushiro, The system forsterite-diopside-silica with and without water at high pressures, *Am. J. Sci.* 267-A, 269, 1969.
- 20 H.J.B. Dick, Partial melting in the Josephine Peridotite, I. The effect on mineral composition and its consequence for geobarometry and geothermometry, *Am. J. Sci.* 277, 801, 1977.
- 21 A.L. Jaques and D.H. Green, Anhydrous melting of peridotite at 0-15 kbar pressure and the genesis of the tholeiitic basalts, *Contrib. Mineral. Petrol.* 73, 287, 1980.
- 22 W.B. Bryan and J.G. Moore, Compositional variations of young basalts in the Mid-Atlantic Ridge rift valley near latitude 36°49'N, *Geol. Soc. Am. Bull.* 88, 556, 1977.
- 23 E.F. Osborn and D.B. Tait, The system diopside-forsterite-anorthite, *Am. J. Sci.*, Bowen Vol., p. 413, 1962.
- 24 W.B. Bryan and H.J.B. Dick, Contrasted abyssal basalt liquidus trends: evidence for mantle major element heterogeneity, *Contrib. Mineral. Petrol.* 88, 287, 1983.

- geneity, *Earth Planet. Sci. Lett.* 58, 15, 1982.
- 25 G.M. Biggar and D.J. Humphries, The plagioclase, forsterite, diopside liquid equilibrium in the system CaO-Na<sub>2</sub>O-Al<sub>2</sub>O<sub>3</sub>-SiO<sub>2</sub>, *Mineral. Mag.* 44, 309, 1981.
- 26 J.-G. Schilling and G. Thompson, Hotspot-MAR interactions and mixing from 80°N to 47°S (abstract), *EOS, Trans. Am. Geophys. Union* 64, 324, 1983.
- 27 W.B. Bryan, Systematics of modal phenocryst assemblages in submarine basalts: petrologic implications, *Contrib. Mineral. Petrol.* 83, 62, 1983.
- 28 A.B. Watts and S. Daly, Long wavelength gravity and topography anomalies, *J. Geophys. Res.* 81, 1533, 1981.
- 29 D. McKenzie, A. Watts, B. Parsons and M. Roufosse, Planform of mantle convection beneath the Pacific Ocean, *Nature* 188, 442, 1980.
- 30 B. Parsons and S. Daly, The relationship between surface topography, gravity anomalies and temperature structure of convection, *J. Geophys. Res.* 88, 1129, 1983.
- 31 H.J.B. Dick and W.B. Bryan, Contrasting abyssal basalt liquidus trends and regional variations in the composition of abyssal peridotites (abstract), *EOS, Trans. Am. Geophys. Union* 64, 310, 1983.
- 32 P.J. Michael and E. Bonatti, Peridotites from DSDP Leg 82 and Oceanographer Fracture Zone (Abstract), *EOS, Trans. Am. Geophys. Union* 64, 345, 1983.
- 33 C.H. Langmuir and G.N. Hanson, An evaluation of major element heterogeneity in the mantle sources of basalt, *Philos. Trans. R. Soc. London, Ser. A*, 27, 383, 1980.
- 34 F.A. Frey, Rare earth element abundances in upper mantle rocks, in: *Rare Earth Element Geochemistry*, P. Henderson, ed., p. 153, Elsevier, Amsterdam, 1984.
- 35 F.A. Frey and D.H. Green, The mineralogy, geochemistry and origin of lherzolite inclusion in Victorian basanites, *Geochim. Cosmochim. Acta*, 38, 1023, 1974.
- 36 G.N. Hanson, Geochemical evolution of the sub-oceanic mantle, *J. Geol. Soc. London* 134, 235, 1977.
- 37 J. Tarney, D.A. Wood, J. Varet, A.D. Saunders and J.R. Cann, Nature of mantle heterogeneity in the North Atlantic: evidence from Leg 49 basalts, in: *2 Deep Drilling Results in the Atlantic Ocean: Ocean Crust*, M. Talwani, C.G. Harrison and D.E. Hayes, eds., *Am. Geophys. Union, Maurice Ewing Ser.* 2, 285, 1979.
- 38 T. Shibata, G. Thompson and F.A. Frey, Tholeiitic and alkali basalts from the Mid-Atlantic Ridge at 43°N, *Contrib. Mineral. Petrol.* 70, 127, 1979.
- 39 G. Thompson, W.B. Bryan and W.G. Melson, Geological and geophysical investigations of the Mid-Cayman Rise Spreading Center: geochemical variation and petrogenesis of basalt glasses, *J. Geol.* 88, 41, 1980.
- 40 J.M. Sinton, Petrology of (alpine-type) peridotites from Site 395, DSDP Leg 45, in: *Initial Reports of the Deep Sea Drilling Project* 45, p. 595, U.S. Government Printing Office, Washington, D.C., 1979.
- 41 F. Aumento and H. Loubat, The Mid-Atlantic Ridge near 45°N, XVI. Serpentinized ultramafic intrusions, *Can. J. Earth Sci.* 8, 631, 1971.
- 42 A. Hofmann and S.R. Hart, The assessment of local and regional isotopic equilibrium in the mantle, *Earth Planet. Sci. Lett.* 38, 44, 1978.